Angewandte Chemie
Eine Zeitschrift der Gesellschaft Deutscher Chemiker

Supporting Information

69451 Weinheim, Germany

Deep-Tissue Photoacoustic Tomography of a Genetically Encoded Near-Infrared Fluorescent Probe**

Grigory S. Filonov, Arie Krumholz, Jun Xia, Junjie Yao, Lihong V. Wang, and Vladislav V. Verkhusha**

anie_201107026_sm_miscellaneous_information.pdf

Table of Contents

Supporting Methods ……... 3
Supporting Figure 1 …… 5
Supporting Figure 2 …… 6
Supporting Figure 3 …… 7
Supporting Figure 4 …… 8
Supporting Table 1 …… 9
Supporting References …… 10

Supporting Methods.

***In vitro* PA studies.** Bacterial plasmids encoding several far-red GFP-like FPs were kindly provided by Benjamin Glick (University of Chicago, USA) and Dmitry Chudakov and Konstantin Lukyanov (both from the Institute of Bioorganic Chemistry, Moscow, Russia). Recombinant GFP-like FPs were expressed in LMG194 bacterial cells and purified using a Ni-NTA agarose (Qiagen). The purified FP solutions were diluted to equal concentrations of 32 μM.

For determining the best FP for PA imaging, a phantom consisted of approximately 20.00 mm long, 0.30 mm inner diameter (i.d.) tubing sections (Silastic Laboratory) filled with one of the FP samples or blood. The tubes were then glued in parallel onto a flat gelatin block and imaged at 600 nm and 680 nm with ~90 mJ incident energy, using a 512 element ring transducer PACT system with top illumination from an OPO laser (Vibrant 335 I)[1]. The wavelengths were chosen to cover wavelengths near the peak excitation of each of FPs. The signal amplitude was compensated for laser power differences using a photodiode signal for normalization, and the signal from each FP was further normalized to blood absorption for comparison.

The depth analysis phantom consisted of approximately 20.00 mm long, 1.47 mm i.d. tubing sections (Silastic Laboratory) filled with either iRFP or blood for comparison. The sections were then embedded in the chicken breast tissue and imaged using deep-PAM, with illumination provided by a Ti-Sapphire laser (LT-2211A) at 700 nm and approximately 100 mJ incident energy[2]. Deep-PAM was used for its reflection mode geometry, allowing for easier simulation of depth imaging. The illumination wavelength of 700 nm enabled delivery of greater laser energy with a similar protein absorption efficiency. Additional depths were simulated by stacking sections of chicken breast tissue on the sample surface. Twenty B-mode images were averaged at each depth. The noise equivalent concentration was calculated by dividing the known concentration of the absorber by the SNR of the sample, and provided an estimate of the expected minimum concentration detectable by the system for this sample.

Mammalian plasmids and cell culture. A pEGFP-C1 vector (Clontech) was utilized to construct plasmids for iRFP mammalian expression and to create a stable line. The iRFP gene was PCR-amplified to have the Kozak sequence on its 5'-terminus and inserted into the *Nhe*I and *Kpn*I sites of the vector, thus generating a piRFP plasmid. The MTLn3 cell line (rat adenocarcinoma) was grown in alphaMEM containing 5% fetal bovine serum (FBS) and penicillin-streptomycin. Plasmid transfection was performed using an Effectene reagent (Qiagen) according to the manufacturer's protocol. Stably-expressing cells were selected with

700 μg/ml G418 antibiotic. Sorting of positive cells was performed using a MoFlo XDP sorter (Beckman Coulter) equipped with a 676 nm Kr laser and a 700 nm LP emission filter. Stably EGFP-expressing and TagRFP657-expressing MTLn3 cells were described previously[3].

***In vivo* fluorescent imaging and PA studies.** One million of the MTLn3 cells stably expressing iRFP, TagRFP657 or EGFP were injected into the mammary gland of SCID/NCr mice (female), and imaged starting one (iRFP) or two weeks (TagRFP657 and EGFP) after that, using an IVIS Spectrum instrument (Caliper Life Sciences) in epifluorescence mode. The IVIS Spectrum instrument was equipped with 675/30 nm and 720/20 nm filters (for iRFP imaging), 605/30 nm and 660/20 nm filters (for TagRFP657 imaging), and 465/30 nm and 520/20 (for EGFP imaging) for excitation and emission, respectively. Belly fur was removed using a depilatory cream. When required, 250 nmol of BV were injected intravenously. iRFP- or EGFP-expressing tumors were excised postmortem. For the FACS analysis using MoFlo XDP, tumors were chopped into pieces, washed with a phosphate buffered solution supplemented with 2% of bovine serum albumin, and subsequently filtered through sieves and FACS filter.

For PACT, two mice were imaged at the tumor region at two weeks and three weeks post inoculation using three wavelengths, 700 nm, 760 nm, and 796 nm. For spectral separation, the images were then processed using a linear least squares method for the three absorbers[4]. For clear separation from blood, the wavelengths were chosen such that absorption by iRFP is near the maximum at 700 nm, and essentially zero at the other wavelengths.

Two and three weeks post injection, a 15 mm by 15 mm area was imaged using the deep-PAM system. Images were taken at the same near-IR wavelengths as the PACT experiment, with depth simulated by stacking approximately 4 mm of the chicken breast tissue over the sample. The same least square method was performed for spectral separation at both depths. To assess the iRFP concentration, we assumed the average total hemoglobin concentration to be similar through the depths imaged, and we normalized the calculated concentrations of iRFP to the average total hemoglobin concentration at each depth. Given the literature value for total hemoglobin concentration of 2.3 mM, the estimated maximum iRFP concentration would then be between 21 to 22 μM.

All animal experiments were performed in an AAALAC approved facility, using protocols approved by the Washington University in St. Louis Animal Use Committee.

Supporting Figure 1. Fluorescent whole-body imaging of the mice 1 week after the injection of the iRFP-expressing cancer cells.

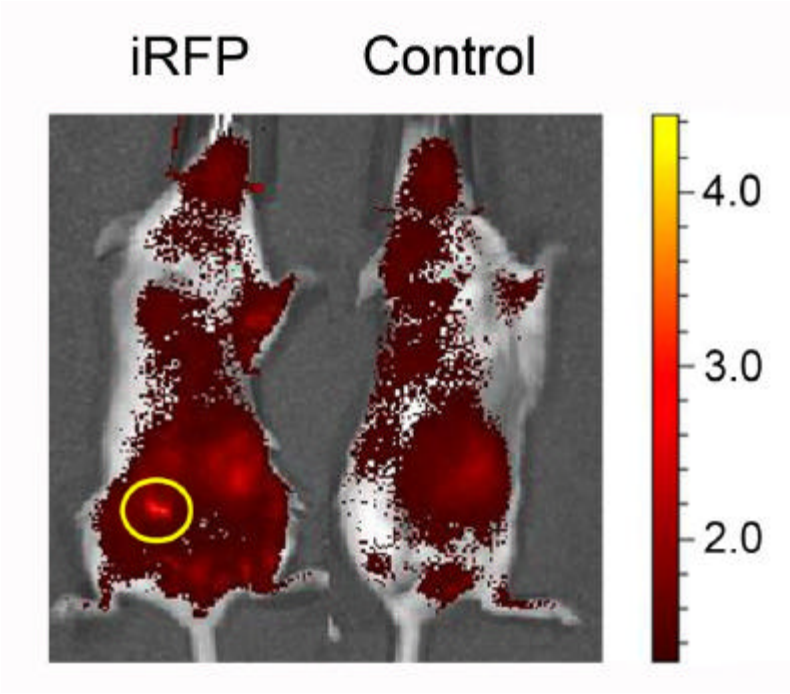

One million of the MTLn3 cells stably expressing iRFP were injected into the mammary gland of SCID/NCr mice and imaged starting one week after that using IVIS Spectrum instrument (Caliper LifeSciences) in epifluorescence mode equipped with 675/30 nm and 720/20 nm filters for excitation and emission, respectively. The belly fur was removed using a depilatory cream. The injection site is shown with yellow circle. The color bar indicates the fluorescence radiant efficiency (p s^{-1} sr^{-1} μW^{-1} cm^{-2}) multiplied by 10^7.

Supporting Figure 2. Direct BV injection into the iRFP-expressing tumor.

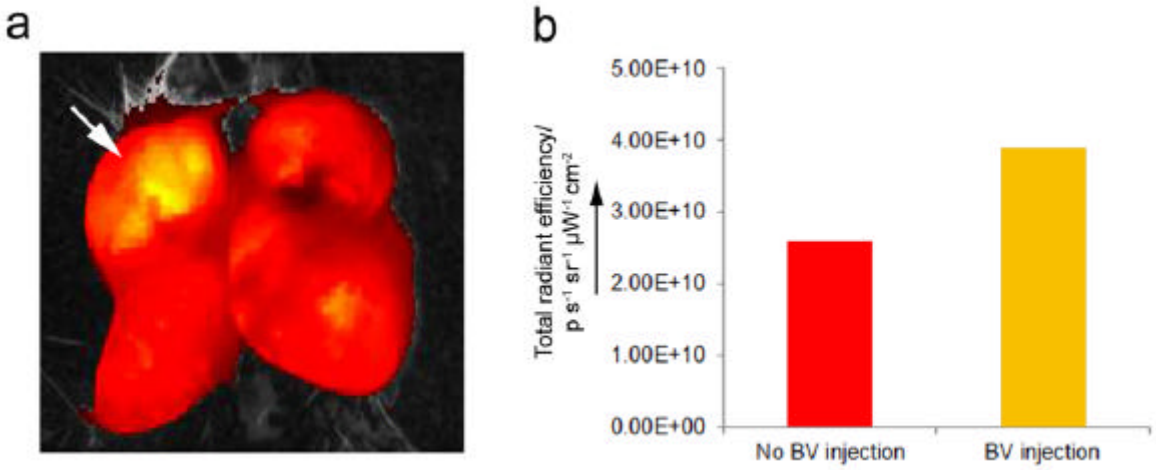

75 nmol BV in DMSO was injected directly into the tumor. The next day the mouse was sacrificed and the tumor was isolated and dissected into the halves (**a**). The injection site (indicated by the arrow) is ~1.5 fold brighter as calculated by measuring of the total radiant efficiency in injected area and non-injected area of the same square (**b**). Non-uniform BV distribution in tumor after direct injection precludes fluorescence brightness-based time-course measurements.

Supporting Figure 3. PACT imaging of the 2 week old iRFP-expressing tumor.

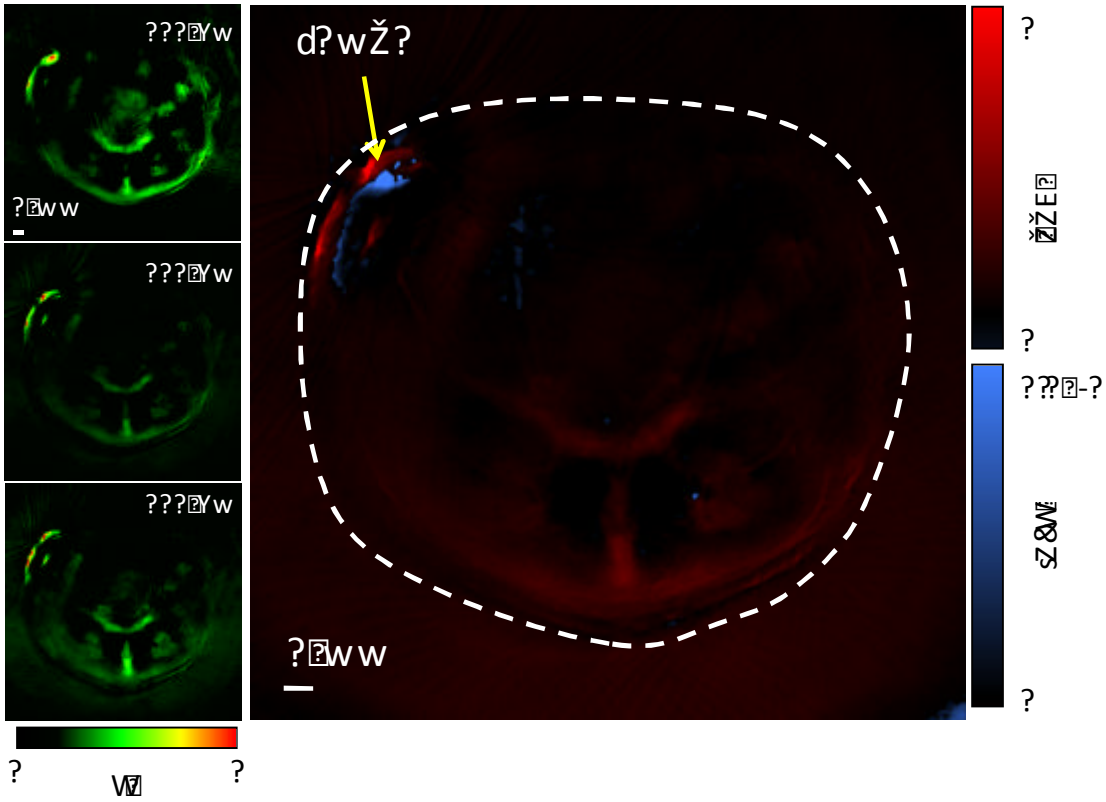

Using the PACT setup described previously, three images on the left were taken at different wavelengths (indicated); the main image is a spectrally separated one, with the tumor in blue and the blood in red. Color bars represent normalized PA amplitude (bottom) or the spectrally resolved iRFP and blood signals normalized to the spectrally resolved blood signal (right). The position of the tumor is labeled with the yellow arrow. The white dashed line shows the mouse body borders.

Supporting Figure 4. Deep-PAM imaging of the cross-section of the 2 week old iRFP-expressing tumor.

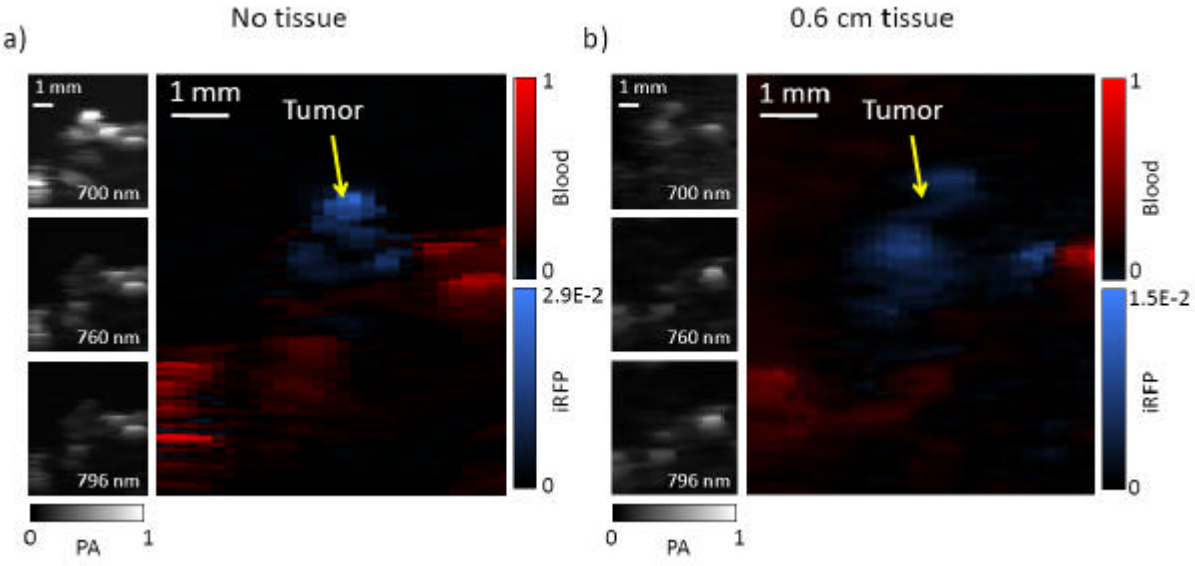

Using the deep-PAM system described previously, three images on the left were taken with no tissue overlay (a) and with 6 mm tissue overlay (b) at different wavelengths (indicated); the main image is a spectrally separated one, with the tumor in blue and the blood in red. Color bars represent normalized PA amplitude (bottom) or the spectrally resolved iRFP and blood signals normalized to the spectrally resolved blood signal (right). The position of the tumor is labeled with the yellow arrow. The white dashed line shows the mouse body borders.

Supporting Table 1. Spectral properties of the fluorescent proteins used in the paper.

FPs	Excitation maximum (nm)	Emission maximum (nm)	Molar extinction coefficient (M^{-1} cm^{-1})	Quantum yield of fluorescence	Molar extinction coefficient **x** Non-radiative quantum yield (M^{-1} cm^{-1})
mKate2[5]	588	633	56,400	0.39	34,404
mNeptune[5]	600	650	59,000	0.20	47,200
eqFP670[6]	605	670	70,000	0.06	65,800
E2-Crimson[6]	605	646	58,500	0.12	51,480
TagRFP657[5]	611	657	34,000	0.10	30,600
iRFP[7]	690	713	105,000	0.06	98,700

Supporting References

[1] J. Gamelin, A. Maurudis, A. Aguirre, F. Huang, P. Guo, L. V. Wang, Q. Zhu, *Optics express* **2009**, *17*, 10489-10498.

[2] K. Maslov, H. F. Zhang, S. Hu, L. V. Wang, *Optics letters* **2008**, *33*, 929-931.

[3] a) C. Xue, J. Wyckoff, F. Liang, M. Sidani, S. Violini, K. L. Tsai, Z. Y. Zhang, E. Sahai, J. Condeelis, J. E. Segall, *Cancer research* **2006**, *66*, 192-197; b) D. Entenberg, J. Wyckoff, B. Gligorijevic, E. T. Roussos, V. V. Verkhusha, J. W. Pollard, J. Condeelis, *Nature protocols* **2011**, *6*, 1500-1520.

[4] D. Razansky, M. Distel, C. Vinegoni, R. Ma, N. Perrimon, R. W. Köster, V. Ntziachristos, *Nature photonics* **2009**, *3*, 412 - 417.

[5] K. S. Morozova, K. D. Piatkevich, T. J. Gould, J. Zhang, J. Bewersdorf, V. V. Verkhusha, *Biophysical journal* **2010**, *99*, L13-15.

[6] D. Shcherbo, Shemiakina, II, A. V. Ryabova, K. E. Luker, B. T. Schmidt, E. A. Souslova, T. V. Gorodnicheva, L. Strukova, K. M. Shidlovskiy, O. V. Britanova, A. G. Zaraisky, K. A. Lukyanov, V. B. Loschenov, G. D. Luker, D. M. Chudakov, *Nature methods* **2010**, *7*, 827–829.

[7] G. S. Filonov, K. D. Piatkevich, L. M. Ting, J. Zhang, K. Kim, V. V. Verkhusha, *Nature biotechnology* **2011**, *29*, 757-761.